Nonlinear localization of light in disordered optical fiber arrays

Gowri Srinivasan[*,†]
Theoretical Division, Los Alamos National Laboratory, Los Alamos, New Mexico 87545, USA

Alejandro Aceves[‡]
Department of Mathematics and Statistics, University of New Mexico, Albuquerque, New Mexico 87131, USA

Daniel M. Tartakovsky[§]
Department of Mechanical and Aerospace Engineering, University of California San Diego, La Jolla, California 92093, USA

(Received 22 February 2008; published 9 June 2008)

Light propagating through optical fiber arrays tends to localize in only a few center cores. The recent experiments in two-dimensional single-mode optical fiber arrays suggest that an interplay of deterministic and random linear and nonlinear effects might be responsible for this localization. We study this phenomenon, both analytically and numerically, in a hexagonal optical fiber array similar to that used in the experiments. Our analysis reveals that Anderson localization is evident in the linear and intermediate regimes, where a larger fraction of initial energy is returned to the center fiber due to the stochastic effects. For very high levels of input energy, the system is strongly nonlinear, with the randomness amplifying the Kerr localization.

DOI: 10.1103/PhysRevA.77.063806 PACS number(s): 42.25.Dd, 42.65.Tg, 72.15.Rn

I. INTRODUCTION

A balance of self-focusing nonlinearity and discrete diffraction due to nearest-neighbor coupling causes localization of light in semiconductor waveguide arrays. This localization takes the form of discrete solitons, a phenomenon that was first confirmed experimentally in [1]. Early attempts to model light propagation in optical arrays dealt with low intensities of input light, for which the effects of nonlinearity can be ignored. This leads to a linear solution for light diffraction given in terms of a Bessel function, which was confirmed experimentally [1,2]. Both this solution and the experiments [1,2] revealed the absence of solitons in such linear systems.

Subsequent experiments (see, e.g., [3]) elucidated the nonlinear effects in uniform and nonuniform waveguides. Solitons were observed only at high intensities of the input light [4]. The formation of solitons is attributed to the Kerr effect, whereby the refractive index of the fiber focuses light so that it balances diffraction. The robustness of the formation of solitons or localization has been verified in relation to the input position in the array [5], angle of incidence [6], and power [4].

These and many other theoretical and experimental studies of nonlinear waveguide arrays dealt with deterministic systems, typically with the waveguides being equally spaced and having identical physical characteristics. In such systems, the coupled discrete nonlinear Schrödinger equation (DNLSE) can be used to model the propagation of the field's complex amplitudes in any given fiber in an array [7,8]. This equation accounts for both discrete diffraction due to weak coupling between neighboring fibers and site nonlinearity due to the intensity-dependent index of refraction. While the DNLSE does not yield a fully integrable system, its continuum approximation does. Since [8], localization in one-dimensional coupled waveguides has been investigated extensively using various analytical and numerical techniques. The significance of localization in signal processing has led to the analysis of collapse-type methods for compressing optical pulses, which localize diffracted energy into just a few fibers in an array [9]. Such methods have been numerically proven to be robust. Beam steering effects have been captured qualitatively using different analytical descriptions of self-trapping solitons [10].

In contrast, localization of energy in the linear regime due to disorder is a fascinating physical phenomenon. Anderson [11] observed localization of energy of electrons moving in disordered atomic crystals. Recent research in photonic systems has explored this phenomenon by combining it with nonlinear effects. For example, nonlinear Anderson localization was observed in one-dimensional [12,13] and two-dimensional [14] disordered photonic lattices, and in general, two-dimensional disordered optical media [15], disordered photonic crystal waveguides [16], and in one-dimensional disordered metamaterials [17]. Specific to nonlinear modes is the analysis of soliton percolation in disordered optical lattices in [18].

The experimental study [19] dealt with light localization due to the effects of nonlinearity and disorder in a fiber array. The disorder (randomness) was caused by the variable separation between cores of different diameters, and quantified in terms of variances in the diameter and coupling distances. Here we present an analytical and numerical analysis of this experiment in order to explain localization resulting from linear, nonlinear, deterministic and random effects in fiber arrays. Attention is paid to two scenarios, deterministic and stochastic. The latter parallels the experimental work by using the same statistics given in [19]. In Sec. II, we present

*Also at Department of Mathematics and Statistics, University of New Mexico, Albuquerque, NM 87131, USA.
†gowri@lanl.gov
‡aceves@math.unm.edu
§dmt@ucsd.edu

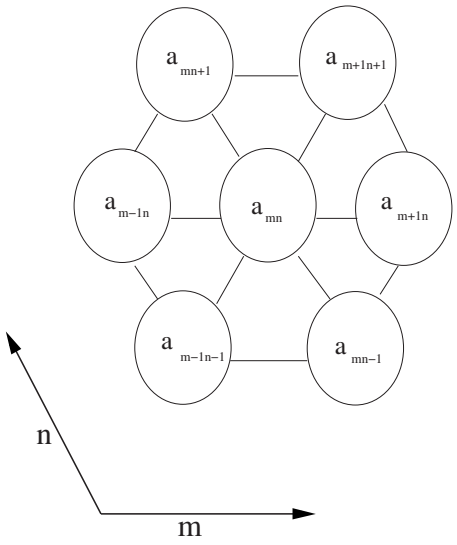

FIG. 1. Schematic representation of the cross section of a disordered hexagonal fiber array: A microscope image of the experimental configuration can be found in Fig. 1 of [19].

the governing equations, summarize what is relevant about the deterministic model, and describe the approach we used to study the effects of stochasticity. Section III contains the description of the numerical algorithms used to solve these equations. In order to verify our numerical solutions, we derive an analytical asymptotic solution for the localization problem in Sec. IV. A discussion of the simulation results is given in Sec. V.

II. GOVERNING EQUATIONS

The experimental study [19] was conducted using a hexagonal optical array consisting of 400 fibers. The cross section of the actual array can be seen in Fig. 1 of [19]; its schematic representation is given in Fig. 1. Each internal fiber in the hexagonal array is surrounded by, and weakly coupled to, six neighboring fibers. In order to mimic the experiment as closely as possible, our analysis considers 12 hexagonal layers, with a total of 397 fibers. The center fiber is referred to as the first layer, the second layer being the six fibers that surround the center fiber, and so on.

Equations for the propagation of light through an optical fiber array are derived from Maxwell's equations by assuming the field to be a superposition of a single transverse mode of the individual core $U(x-x_{m,n},y-y_{m,n})$, where $(x_{m,n},y_{m,n})$ are transverse coordinates of the location of the (m,n) fiber. A governing equation for $a_{m,n}$, the amplitude in the (m,n) fiber, is derived by using the weakly nonlinear theory. It is a generalization of Jensen's model for the directional coupler [20], wherein the balance of Kerr nonlinearity and the coupling due to the presence of the tail of the mode (m,n) at the neighboring sites results in a system of complex ordinary differential equations (ODEs) [19],

$$\left(i\frac{d}{dz}+\beta_{m,n}+\chi|a_{m,n}|^2\right)a_{m,n}+c_{m,n}(a_{m+1,n}+a_{m-1,n}+a_{m,n+1}+a_{m+1,n-1}+a_{m+1,n+1}+a_{m-1,n-1})=0. \quad (1)$$

Here $i=\sqrt{-1}$; z is the scaled coordinate describing propagation distance; $c_{m,n}$ is the strength of the nearest-neighbor coupling, which is proportional to the separation between cores; $\beta_{m,n}$ is the propagation constant, which depends, among other things, on the fiber core diameter; and χ is the nonlinear coefficient assumed to be constant.

After reindexing each core (m,n) with a single index k, Eq. (1) can be written as

$$i\frac{da_k}{dz}=-\beta a_k-c\sum_j a_j-\chi|a_k|^2a_k, \quad (2)$$

where the summation is over neighboring fibers. Here the terms involving the propagation and coupling constants are linear while that involving χ is nonlinear (cubic) in nature. Writing similar equations for each fiber in the array gives rise to a system of equations that can be represented as a vector equation for $\tilde{a}=[a_1a_2,\ldots,a_N]'$, where N is the total number of fibers.

$$i\frac{d\tilde{a}}{dz}=(L+N)\tilde{a}, \quad (3)$$

where the terms in any row k of the linear matrix (L) are β in column k corresponding to the same fiber, c in the columns corresponding to immediate neighbors, and zero otherwise. The nonlinear matrix (N) is a diagonal matrix with term $N_{k,k}=\chi|a_k|^2$.

Representing the complex amplitude a_k as $a_k=x_k+iy_k$, one obtains two real ODEs that jointly describe the propagation of the amplitude of light along the fiber's length.

A. Deterministic case

The most extensively studied model assumes that all fibers in the array are identical and perfectly stacked. This implies that propagation constant β has the same value for each fiber, and the coupling constant c between every fiber and its immediate neighbors is the same. Then Eq. (2) reduces to

$$\frac{dx_k}{dz}=-y_k[\beta+\chi(x_k^2+y_k^2)]-c\sum_j y_j,$$

$$\frac{dy_k}{dz}=x_k[\beta+\chi(x_k^2+y_k^2)]+c\sum_j x_j. \quad (4)$$

Following recent experiments [19], we consider a scenario in which light is initially incident through the center fiber only and analyze the intensity distribution at the output as a function of the incident power at the single site. Then the hexagonal symmetry of the fiber array implies that all fibers in a given layer with the same number of immediate neighbors behave identically. Additionally, already built into the model is an assumption of an ideal system with no losses, so that the total energy in all the fibers must remain constant over the propagation length.

Since light enters the array through the center fiber only, its intensity in each fiber has a quasiperiodic z dependence, with periods depending upon both the initial input energy and the number of hexagonal layers considered in the model.

This is because the model represents a high-dimensional Hamiltonian system with regions of quasiperiodic behavior. In the linear regime, the input light is expected to diffract to the outer layers without revisiting the input fiber. However, for high enough powers, experimental results show that the spread of energy is confined to only a few layers and that energy flows back into the input fiber, leading to the possibility of localization [19].

There also exists a stationary state (z-independent) solution for this system of optical fibers that can be approximated by an asymptotic expansion. The asymptotic stationary solution is said to be localized if most of the initial input energy remains in the center fiber. The robustness of the asymptotic localized stationary solution, in the sense that the dynamics stays close to such a state, varies with the total energy. We discuss this point further, and analyze the effects of randomness on localization in later sections.

The localization of light entering the array through the center fiber is measured in terms of the fraction of the total energy that propagates in the center fiber. The energy in the center fiber is sampled as a fraction of the total energy at numerous randomly chosen lengths along the propagation direction close to the exit. Such a sampling gives a frequency distribution of energy states that are visited in the input fiber. While the system is fully deterministic, presenting the results in this fashion facilitates a comparison with the case in which randomness is included.

B. Stochastic model

Due to manufacturing imperfections that cannot be quantified in all of their relevant details, fiber array systems have inherent stochasticity. In other words, the propagation term that depends upon the diameter of the optical fiber varies randomly about a given mean due to the uncertainties involved in the fabrication process. The coupling depends upon the core spacing, which also varies randomly due to errors during stacking of the fiber optic array. Both quantities can be represented as the sums of their respective mean values β_0 and c_0 and random fluctuations $\delta\beta$ and δc that are assumed to be Gaussian,

$$\beta = \beta_0 + \delta\beta, \quad c = c_0 + \delta c. \tag{5}$$

We consider the conceptual representation of randomness as studied experimentally in [19], where both the coupling between fibers and the propagation constant of each fiber have been chosen randomly from Gaussian distributions whose means and variances reflect experimental data. For each realization of random constants β and c, the governing ODEs remain deterministic, but since their values differ from one fiber to another, the hexagonal symmetry is no longer preserved.

The key difference between the deterministic and stochastic representations is that the latter results in the dynamics that is no longer strictly periodic. However, a periodic-like behavior with a random period and random amplitude can still be seen. Possible localization is determined by analyzing a sampling of the energy fraction in the center fiber, which is now performed on the average energy of multiple Monte Carlo realizations. The sampling is carried out in the same way as in the deterministic case at randomly chosen lengths along the propagation direction.

III. COMPUTATIONAL APPROACH

The fiber optic array studied [19] had a coupling constant with mean 46 m^{-1} and standard deviation 26.7 m^{-1}, and a propagation constant with mean 11.4×10^6 m^{-1} and standard deviation 140 m^{-1}. Randomness in the nonlinearity was disregarded. A change of variables and the subsequent nondimensional analysis yielded the following values: $\beta_0=0$, $c_0=1$ and $\chi=1.1$.

The mean values of these properties are used to obtain deterministic solutions. Simulations of the experimental stochastic scenario use random values that are drawn from a Gaussian distribution with the corresponding means and variances. For the fiber length considered in the experiments, no significant longitudinal variations of the parameters were observed. In both of these cases, the equations solved are nonlinear ODEs.

A formal solution of the ODE (3) at $z+\Delta z$ can be written as

$$\tilde{a}(z+\Delta z) = e^{-i\Delta z(L+N)}\tilde{a}(z), \tag{6}$$

whose numerical approximation is

$$\tilde{a}(z+\Delta z) \approx e^{-i\Delta z L/2}\vec{d}(z), \tag{7}$$

where

$$\vec{d}(z) = e^{-i\Delta z N}\vec{b}(z) \quad \text{and} \quad \vec{b}(z) = e^{-i\Delta z L/2}\tilde{a}(z). \tag{8}$$

Equation (7) is an approximation, since the operators L and N do not commute. Splitting the solution of the linear portion into two steps of $\Delta z/2$ results in a total error of the order of $(\Delta z)^3$.

The two linear steps in Eq. (7) are solved using the implicit midpoint rule, which conserves quadratic invariants, in this case the total energy. For the first linear step, the implicit midpoint rule yields

$$\vec{b}(z) = \vec{a}(z) + \frac{\Delta z}{2} L\left[\frac{\vec{a}(z)+\vec{b}(z)}{2}\right]. \tag{9}$$

An analogous expression holds for the second linear step. Solution of the nonlinear part of Eq. (7) is facilitated by noting that $N=\boldsymbol{\chi}|\tilde{a}_k|^2$, where $\boldsymbol{\chi}=\chi\mathbf{I}$ is the constant deterministic nonlinearity matrix whose entries represent the nonlinearity coefficients χ for each fiber, and $\mathbf{I}$ is an identity matrix. An analysis of the equations for $\tilde{a}_k$ and its complex conjugate reveals that $|\tilde{a}_k|^2$ is constant and hence the nonlinear part of the equation admits an exact solution.

Note that L is the random linear matrix whose entries represent the random propagation β and coupling coefficients c for each fiber drawn randomly from Gaussian distributions. We will show in Sec. VI that the implicit midpoint rule is identical to the Stratanovich scheme of numerical integration for stochastic differential equations (SDEs), with random values of the coupling (c) and propagation (β) con-

stants generated at each step Δz. This ensures both that the total error in numerical integration is the same as that of the linear part and that the total energy is conserved.

The main goal of this work is to extract information on whether localization occurs. The energy in the fibers varies with the propagation length. We illustrate this by plotting the energy in the center fiber for various initial conditions, i.e., levels of input in the center fiber. The initial energy is input in the center fiber entirely. The values of energy chosen can be classified into linear, nonlinear, and intermediate regimes. The different regimes, as the names indicate, denotes the dominant terms in the governing equation for energy propagation through the fiber. The intermediate regime is one where both linear and nonlinear terms contribute similarly to the propagation of energy through the fiber. In this case, the values of initial input energy lie between the two aforementioned regimes. The results for both deterministic and stochastic scenarios are plotted together for ease of comparison.

An immediate effect of introducing disorder is that it breaks the symmetry. It is expected that fibers in a given layer with the same number of neighbors behave identically in the deterministic case, whereas their behavior in the case of varying properties is quite different. Localization is said to occur based on the fraction of total energy that is retained in the center fiber.

In the deterministic case, the energy in the center fiber is sampled as a fraction of the total energy at 1000 randomly chosen lengths along the propagation direction. This sampling allows one to ascertain which energy states are visited and how often. The sampling lengths are restricted to one period's length before the exit. In the stochastic cases, the average energy of multiple Monte Carlo realizations is sampled. This sampling strategy enables one to both preserve ergodicity and provide a means of comparison between the two models. Comparison of the energy distributions in the center fiber in the deterministic and stochastic cases provides insight into the effects of randomness on localization. Distributions of energy fractions, ranging from 0 to 1, are presented via histograms with a bin size of 0.05. The shape and structure of these histograms shed light on the dynamics of the system and the possibility of localization, as will be seen in the discussion of results in Sec. V.

IV. ASYMPTOTIC LOCALIZED STATIONARY SOLUTIONS

Asymptotic localized solutions are stationary-state solutions of the deterministic system in which a high fraction of the energy input in the center fiber stays in the center fiber, while the remaining energy is distributed across the remaining fibers according to some approximation. We derive the first- and second-order approximations of such asymptotic solutions and check their stability as a function of energy.

Let a_0 denote the amplitude in the center fiber, a_1 denote the amplitude in the fibers in the second layer, and so on. Performing a change of variables and setting $\beta_{m,n}=0$ allows us to rewrite the governing equation (1) for the center fiber in terms of a_0 and a_1 as

$$\left(i\frac{d}{dz}+\chi|a_0|^2\right)a_0+6ca_1=0. \tag{10}$$

A localized solution implies that $|a_0|\gg|a_1|\gg|a_2|$, etc. and that $|a_k|\gg 1$ for $k=0$ and $|a_k|<1$ for $k>0$. In particular, stationary (in intensity) localized states correspond to solutions of the form

$$a_k(z)=a_k e^{i\lambda z}, \tag{11}$$

where all intensities $|a_k|$ are constant. Rather than finding such solutions numerically, we present an asymptotic analysis that illustrates the features of these solutions. If we assume that most of the energy is concentrated in the central fiber, its first-order approximation $a_0^{(1)}$ satisfies an algebraic equation

$$-\lambda a_0^{(1)}+\chi|a_0^{(1)}|^2a_0^{(1)}=0, \tag{12}$$

which is obtained by neglecting terms containing a_1 in Eq. (10). The corresponding solution is

$$a_0^{(1)}=\sqrt{\frac{\lambda}{\chi}}. \tag{13}$$

The first-order approximation of the amplitude in the layer of fibers immediately surrounding the center fiber, $a_1^{(1)}$, satisfies an algebraic equation

$$-\lambda a_1^{(1)}+ca_0^{(1)}=0, \tag{14}$$

which is obtained from Eq. (10) by assuming $\lambda\gg c$ and neglecting the lower-order nonlinear terms and the terms that contain a_2 and a_3. This gives

$$a_1^{(1)}=\frac{a_0^{(1)}}{\lambda}. \tag{15}$$

An equation for the second-order approximation of the amplitude in the center fiber, $a_0^{(2)}$, can be computed from Eq. (10) by including the terms proportional to $a_1^{(1)}$,

$$-\lambda\left[a_0^{(1)}+a_0^{(2)}\right]+\frac{6c}{\lambda}a_0^{(1)}+\chi\left[a_0^{(1)}+a_0^{(2)}\right]^3=0. \tag{16}$$

Neglecting the higher-order terms, we obtain an expression for the second-order approximation of the amplitude in the center fiber,

$$a_0^{(2)}=\frac{6c}{\lambda}\frac{a_0^{(1)}}{\lambda-3\chi[a_0^{(1)}]^2}. \tag{17}$$

A second-order asymptotic approximation is the sum of the first- and second-order approximations, $a_0^{\text{asym}}=a_0^{(1)}+a_0^{(2)}$.

V. RESULTS

The numerical results presented in this section are for a 12-layer hexagonal optical fiber array. This is a system of 397 fibers, where each fiber is surrounded by six immediate neighbors except in the outermost layer. We consider the deterministic scenario, where all fibers are assumed to have identical properties and are equally spaced, and the stochas-

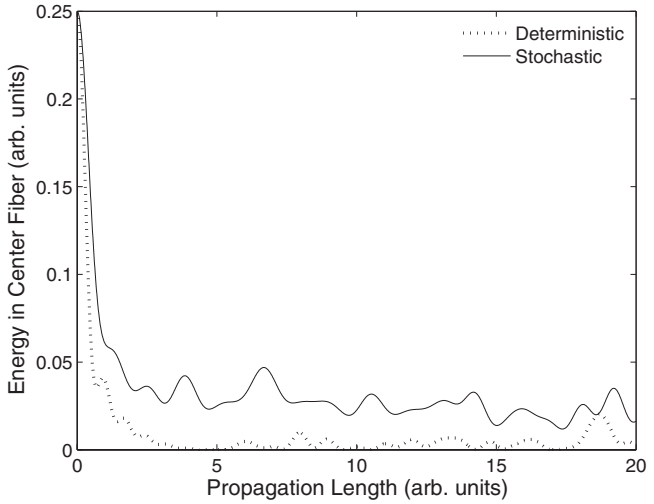

FIG. 2. Propagation dynamics in center fiber: linear input.

tic scenario, which is identical to the experimental setup in [19]. The randomness is in the transverse direction only. The coupling constants between fibers and the propagation constant along each fiber are randomly generated using the mean and standard deviation values documented by the manufacturer. These values are assumed to be constant over the length of propagation, in this case 40 cm. Numerical simulations were performed for both of these cases.

The propagation dynamics in the center fiber is quantified by the amount of energy as a function of fiber length. The results for the deterministic case are plotted alongside the averaged results in the stochastic case for the purpose of comparison (Figs. 2–5). As one can clearly see, randomness inhibits the quasiperiodic behavior observed in the deterministic case. The presence of linearlike modes is due to symmetry-breaking random defects. For each of the different levels of input, the mean value of energy in the center fiber in the deterministic case is consistently lower than the steady value achieved in the stochastic cases. It can then be said that not only does stochasticity enhance reaching a localized state, it is also with a higher degree of localization. Histograms are used to quantify localization in terms of the distribution of energy in the center fiber as fractions of the total energy. Since the system exhibits distinctly different behaviors depending upon the input intensity, we analyze the results for each of the energy regimes.

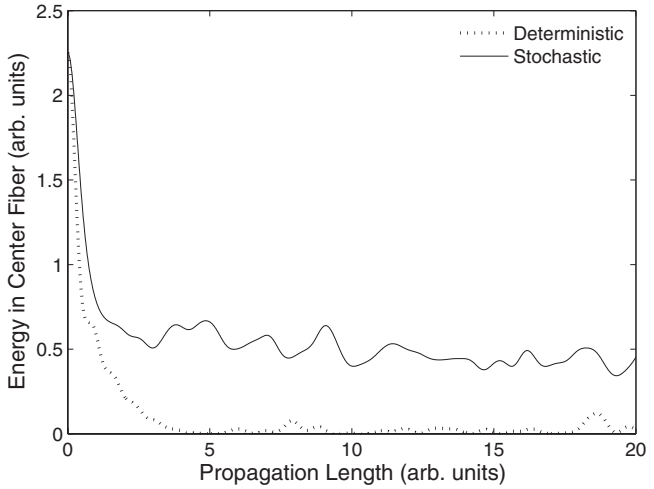

FIG. 3. Propagation dynamics in center fiber: intermediate input.

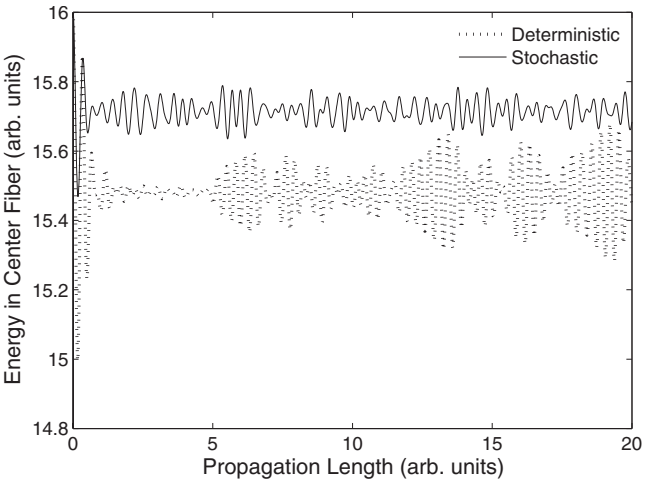

FIG. 4. Propagation dynamics in center fiber: nonlinear input.

A. Linear regime

For input energy levels below 1, the cubic nonlinear term in the governing equation is negligible compared to the coupling terms, which are more dominant. This favors discrete diffraction of the energy from the center fiber to outer layers. There is no significant localization due to the very weak nonlinearity. In both deterministic and stochastic cases, the dynamics shows that only a small fraction of initial input energy is retained in the center fiber (Fig. 2). The averaged stochastic model exhibits a higher level of energy as compared to the deterministic model. It is notable that even at very low input powers such as 0.25 illustrated here in Fig. 2, the randomness plays a significant role in favoring localiza-

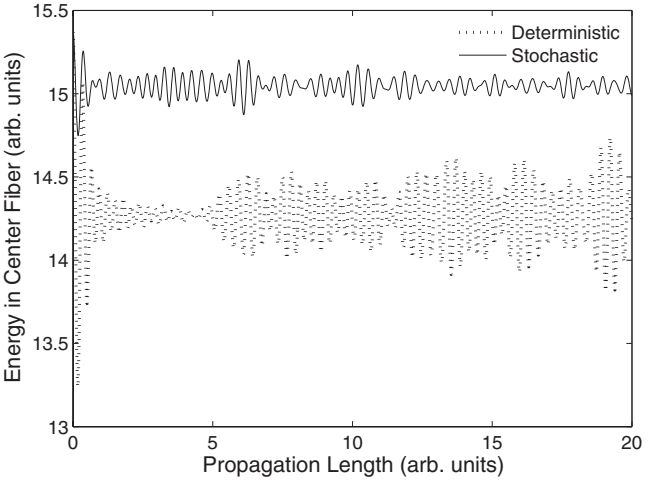

FIG. 5. Propagation dynamics in center fiber: asymptotic localized stationary state.

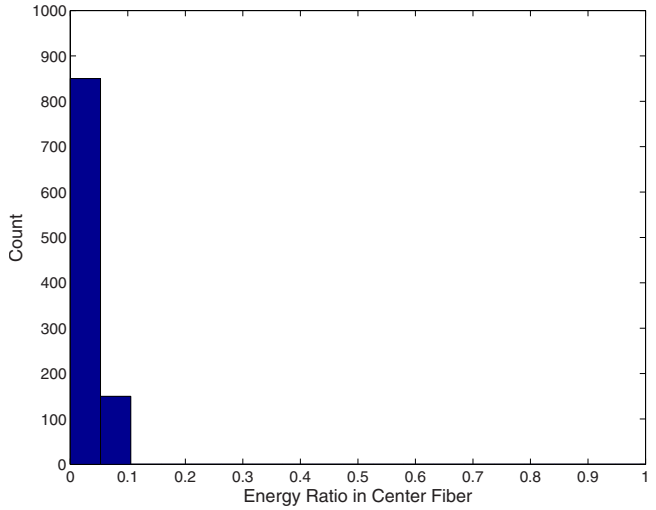

FIG. 6. (Color online) Histogram for linear input in center fiber: Deterministic case.

tion. The histograms provide a quantitative method to compare the fraction of energy retained in the center fiber. In the deterministic case, the histogram shows a single peak very close to 0. Figure 6 shows an example of such behavior for the initial energy input of 0.25. Delocalization is clearly observed, with the lower fractions of energy representing the states visited most often. Most of the initial input energy in the center fiber disperses to the outer layers, with less than 10% of the total energy remaining in the center fiber. The stochastic model (Fig. 7) shows the presence of a pronounced peak in the histogram away from 0 showing a tendency to localize. The fraction of energy retained in the center never falls below 5% but it is less than 15%. Since the phenomenon witnessed here is likely due to Anderson localization, this can be verified by plotting the energies at the exit for each layer of fibers. This is achieved by starting at the center fiber and moving outwards in any one direction to the outermost layer (Fig. 8). The phenomenon of Anderson localization is characterized by an exponential drop off in

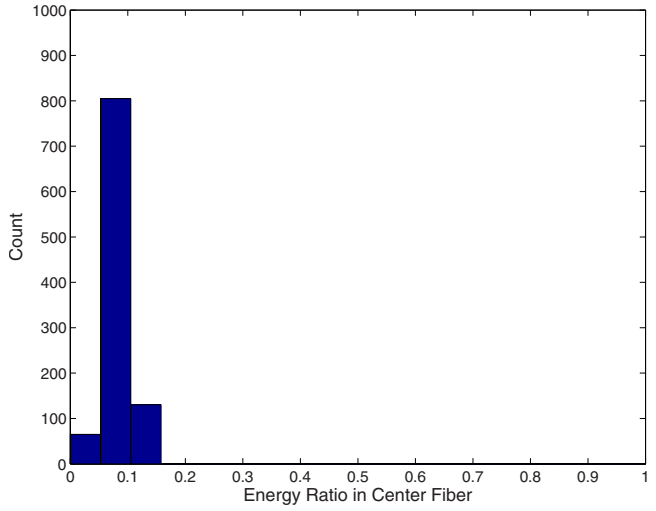

FIG. 7. (Color online) Histogram for linear input in center fiber: Stochastic case.

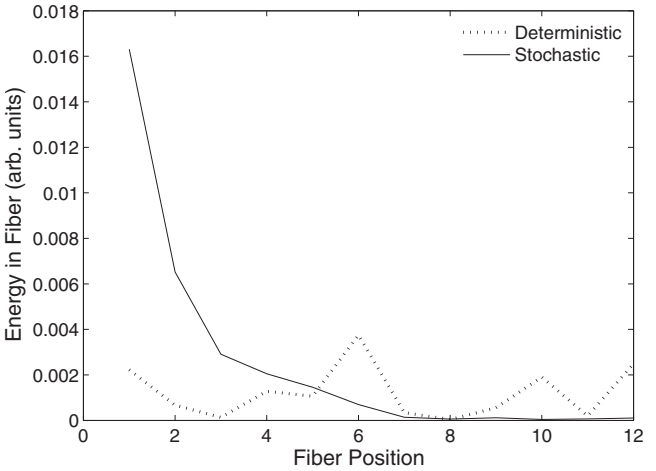

FIG. 8. Energy drop off in transverse direction: Linear input.

energy along the transverse direction, which is clearly seen from the center fiber outwards to layer 8. The behavior in the outermost layers is inconclusive due to the effects of reflection from the outer layers, which sends energy back to the inner layers due to the finiteness of the model. The first eight layers do not experience any significant reflection and exhibit an exponential decay in energy in the transverse direction. We conclude that in the linear regime, though the nonlinearities credited with self-focusing properties are negligible in this case, the localization induced by randomness is observed.

B. Nonlinear regime

At high levels of input energy, above 2, the cubic nonlinear terms are more dominant over the linear coupling terms. This is the highly nonlinear regime, where Kerr effects lead to significant localization. Since it is also seen that stochasticity favors localization in the linear regime, one of the goals was to study the competing effects of both nonlinearity and randomness on localization. While each enhances localization independently, it is interesting to see whether their combined behavior cancels or enhances localization.

The deterministic model of the energy dynamics reveals significant localization (Fig. 4) for an input energy of 16. Just as in the linear regime, the averaged stochastic model exhibits a slightly higher level of energy as compared to the deterministic model. Hence randomness is shown again to increase the localization over and above the nonlinearity.

The histogram of energy fraction in the center fiber is shown in Figs. 9 and 10 for the deterministic and stochastic cases, respectively. These figures demonstrates that the localization always takes place. The histogram is narrow in shape and exhibits a single peak close to the ratio of 1. The fraction of energy in the center input fiber never drops below 95%. This is in sharp contrast with the linear regime in Figs. 6 and 7. The nonlinearity has a much stronger role in localization at these high levels of input energy. However, the role of the random effects is to enhance the already present Kerr localization.

C. Intermediate regime

The region in between the linear and highly nonlinear regions is one of transition. Both the coupling and nonlinear

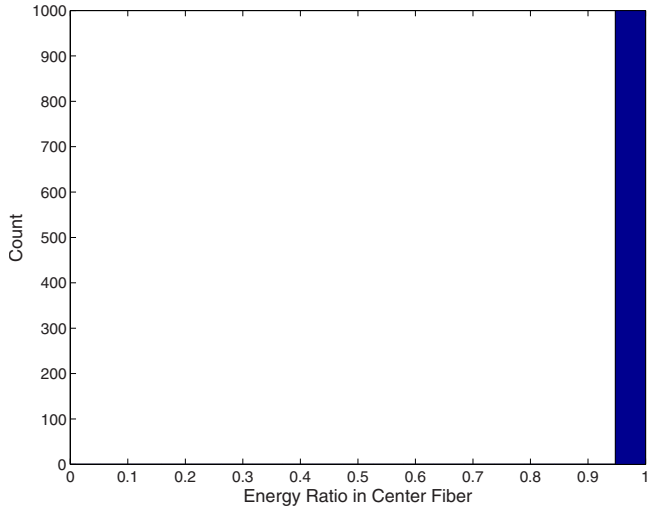

FIG. 9. (Color online) Histogram for nonlinear input in center fiber: Deterministic case.

terms play a significant role in the propagation dynamics. The inclusion of randomness once again increases localization, as the energy retained in the center fiber is higher than in the deterministic case (Fig. 3). For an initial energy input of 2.25, the histogram (Fig. 11) looks similar to that in the linear regime (Fig. 6) for the deterministic case. In this case too, most of the initial input energy in the center fiber disperses to the outer layers, but up to 15% of the total energy remains in the center fiber. The stochastic model, however, shows a significantly higher level of localization than in the linear regime. In Fig. 12, the fraction of energy retained in the center stays between 15% and 25% of the total energy. As the input energy in the center fiber is increased, the histograms of the fraction of energy in the center fiber are skewed closer toward 1, which shows that localized states begin to be favored. Above a certain energy level (say, 4), there is some localization. The peaks in the histogram start shifting toward 1.

Since the stochastic effects on localization are significant in the regime, just like in the linear regime, the question of

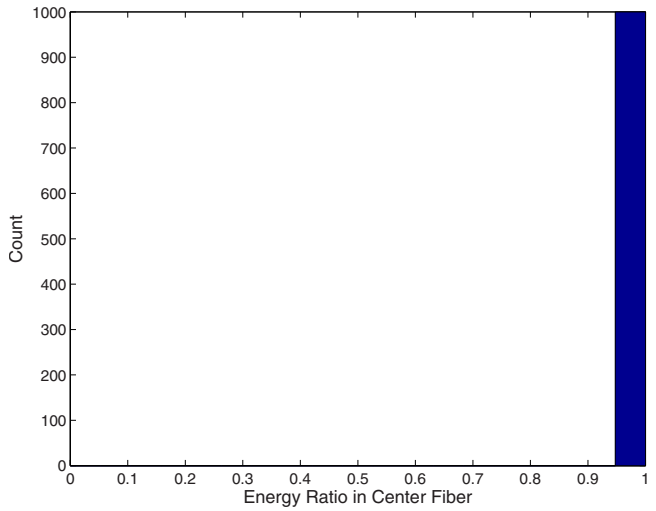

FIG. 10. (Color online) Histogram for nonlinear input in center fiber: Stochastic case.

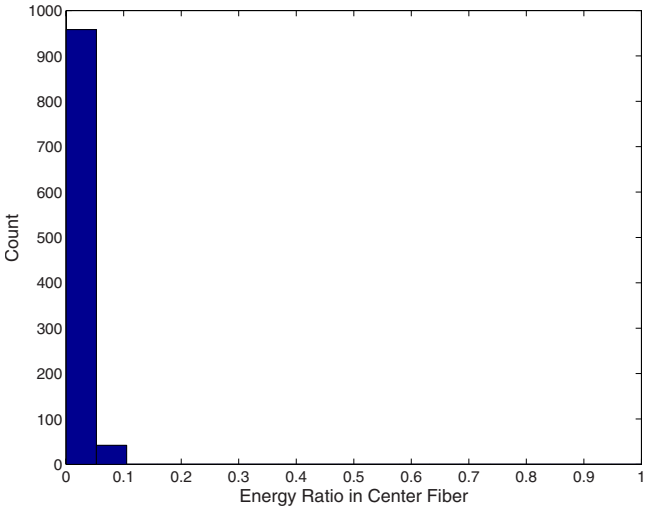

FIG. 11. (Color online) Histogram for intermediate input in center fiber: Deterministic case.

whether Anderson localization holds here is verified by plotting the energies in all the layers at exit. Once again, the transverse drop off in energy is noted (Fig. 13) from the center fiber outwards to layer 7. Since the energies are higher in this case in comparison with the linear regime, so are the reflection effects on the outermost layers. It can be conclusively said that stochasticity plays a significant role in the intermediate regime favoring localization. The behavior exhibited is characteristic of Anderson localization.

D. Asymptotic localized state

One of the effects of including randomness in the model is the existence of a preferred state, giving rise to histograms that are nearly Gaussian. This behavior characterizes both the intermediate energy levels where localization is observed and the highly nonlinear regions. The randomness accentuates the localization effect by picking an asymptotically sta-

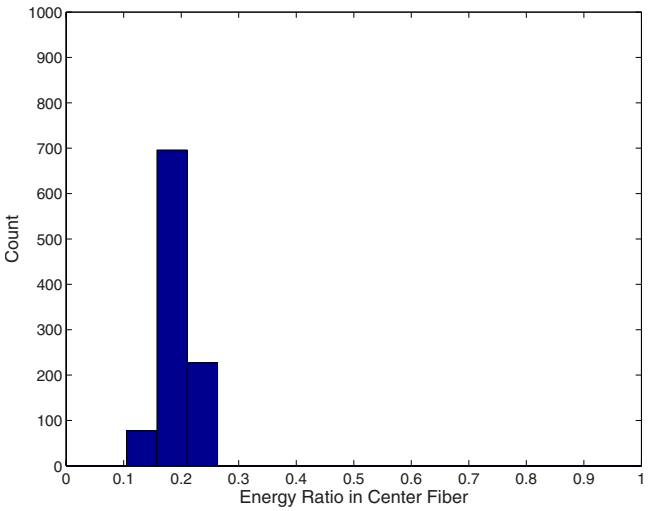

FIG. 12. (Color online) Histogram for intermediate input in center fiber: Stochastic case.

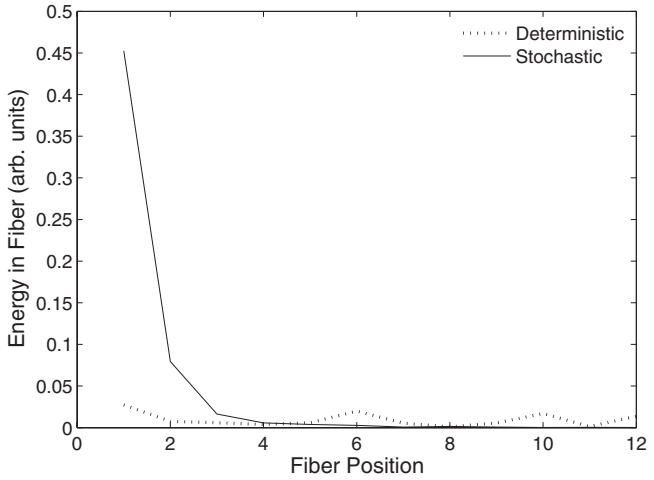

FIG. 13. Energy drop off in transverse direction: Intermediate input.

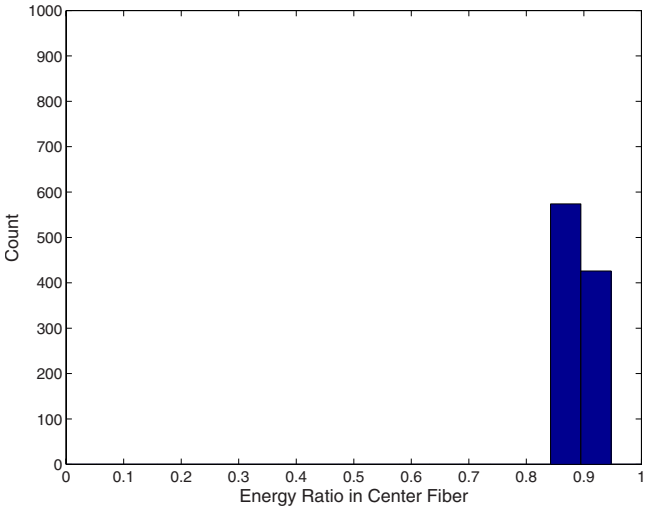

FIG. 14. (Color online) Histogram for asymptotic stationary input in center fiber: Deterministic case.

tionary localized solution. These are nontrivial stationary-state solutions of a high-dimensional stochastic Hamiltonian system. They can be approximated by stationary-state solutions of the corresponding deterministic system with input power distributed uniformly throughout all fibers. This behavior is not observed in the deterministic case.

The asymptotic approximation can be viewed as a perturbation of the exact stationary solution. The localized states and eigenvalues of the approximation are functions of the total energy. With increased energy levels, the perturbations become more stable. Following the calculations in Sec. IV, the asymptotic solution corresponding to a total energy of 16 is computed. This value of initial input energy is chosen so as to be able to compare it with the behavior in the nonlinear regime with pulse input. The initial conditions for this case have a total energy of 15.38 in the center fiber. The energy in each of the fibers in the first layer surrounding the center fiber is 0.053 and the energy in each fiber in the second layer is 0.026. No energy is input through the outer layers.

The propagation dynamics are plotted in Fig. 5. It is remarkable that the asymptotic localized stationary state is observed in the stochastic case, whereas in the deterministic case, the solution is only localized and not stationary. The energy in the stochastic case shows very little variation about the stationary state. The histogram of energy fraction in the center fiber is shown in Figs. 14 and 15 for the deterministic and stochastic cases, respectively. It is clear that while localization always takes place (since over 85% of the energy is always retained in the center fiber), the stationary state solution is only characteristic of the stochastic model. Plotting the energies into finer bins, it can be seen that the fraction of energy in the center input fiber never drops below 97%. In other words, the asymptotic approximation of a stationary solution is valid in the nonlinear regime for the stochastic model.

VI. FUTURE WORK: NONSTATIONARY MODEL

The stochastic model considered in this study so far took into account randomness in the transverse direction only, i.e., properties varied between fibers, but remained constant along the length of each fiber. While this approximation holds for sufficiently small lengths (under 40 cm) of fiber, it is also interesting to consider properties varying along the length of each fiber, in addition to the variation between fibers. This analysis gives rise to a system of SDEs. The governing equations look similar to Eq. (4), with the only difference being that the x_k and y_k are now random variables.

To gain physical insight into the process of localization, while keeping the analysis tractable, we derive an analytical solution for the simplified model (Fig. 1) consisting of seven fibers, i.e., only one layer surrounding the center fiber. Such a model has 14 dimensions. This is in contrast with the full model considered in previous sections, which has 794 dimensions.

The system of 14 SDEs constitute a multivariable nonlinear Langevin system. Consider a Wiener process $W(t)$ with Gaussian increments $\omega(t)$. We use Stratanovich calculus [21,22] to evaluate integrals of the form $\int_0^t \phi(\omega(\tau),\tau)dW(\tau)$,

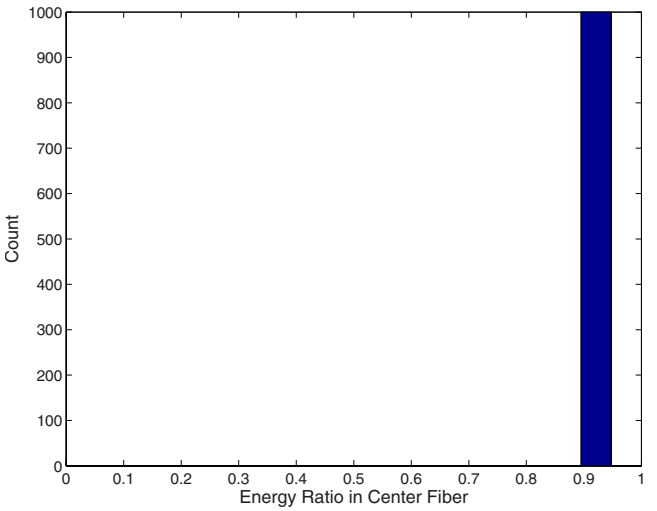

FIG. 15. (Color online) Histogram for asymptotic stationary input in center fiber: Stochastic case.

where $\phi(\cdot)$ is an arbitrary integrable function of $\omega(t)$. The Stratanovich scheme of integration represents this integral by

$$\int_0^t \phi[\omega(\tau),\tau]dW(\tau) = \sum_{i=0}^{N-1} \phi\left(\omega\left(\frac{\tau_i+\tau_{i+1}}{2}\right),\frac{\tau_i+\tau_{i+1}}{2}\right) \times[\omega(\tau_{i+1})-\omega(\tau_i)]. \quad (18)$$

Note that this representation is analogous to the implicit midpoint numerical scheme presented in Sec. III.

The Fokker-Planck equation for the joint probability distribution function (PDF) $P(\vec{x},z)$ of light amplitudes in the seven-fiber system has the form [22]

$$\frac{\partial P}{\partial z} + \sum_{i=0}^{13} \frac{\partial}{\partial \tilde{x}_i}\left(D_i P - \sum_{j=0}^{13} \frac{\partial}{\partial \tilde{x}_j} D_{i,j} P\right) = 0. \quad (19)$$

Here D_i $(i=0,\ldots,13)$ and $D_{i,j}$ $(i=0,\ldots,13;\ j=0,\ldots,13)$ are the so-called drift and diffusion coefficients. The diffusion coefficients form a symmetric positive definite 14×14 matrix. All coefficients have been computed analytically. A few of them are shown below,

$$D_1 = -\chi\tilde{y}_1[\tilde{x}_1^2+\tilde{y}_1^2] - c(\tilde{y}_0+\tilde{y}_2+\tilde{y}_3) - 6\tilde{x}_1,$$
$$D_{1,1} = 2(\tilde{y}_0^2+\tilde{y}_2^2+\tilde{y}_3^2). \quad (20)$$

One can verify that the evolution of average energy $E_i = \langle x_i^2+y_i^2\rangle$ of any fiber i depends only on the second moments of the amplitudes in all fibers. For example, the average energy in the center fiber $(i=0)$

$$\frac{d\langle x_0^2+y_0^2\rangle}{dz} = 2\sum_{i=1}^{6}\langle x_i^2+y_i^2\rangle - 12\langle x_0^2+y_0^2\rangle. \quad (21)$$

Since the neighbors of fiber 1 are fibers 0, 2, and 3, the average energy in the outer layer evolves according to the equation

$$\frac{d\langle x_1^2+y_1^2\rangle}{dz} = 2\langle x_0^2+y_0^2\rangle + 2\langle x_2^2+y_2^2\rangle + 2\langle x_3^2+y_3^2\rangle - 6\langle x_1^2+y_1^2\rangle. \quad (22)$$

It is easy to see that the average total energy $E_{\text{tot}} = \Sigma_i\langle x_i^2+y_i^2\rangle$ is constant.

However, equations that describe evolution of mixed second moments, e.g., $\langle x_i y_j\rangle$ contain higher-order moments and hence require a closure approximation. For example, an equation for $\langle x_1 y_2\rangle$ is

$$\frac{d\langle x_1y_2\rangle}{dz} = c[\langle x_1x_4\rangle + \langle x_1^2\rangle + \langle x_1x_5\rangle - \langle y_4y_2\rangle - \langle y_2^2\rangle - \langle y_2y_3\rangle - \langle y_2y_5\rangle - \langle y_2y_6\rangle - \langle y_2y_7\rangle] - 22\langle x_1y_2\rangle \times\chi[\langle x_2x_1y_2^2\rangle + \langle x_2^3x_1\rangle + \langle x_1^2y_2y_1\rangle + \langle y_2y_1^3\rangle]. \quad (23)$$

Consider localized solutions, where energy in the second layer is negligible compared to that in the center fiber. The total energy in the system E_{tot} remains constant, while the average energy in each of the fibers in the second layer is identical due to the hexagonal symmetry. This leads to equations describing evolution of average energy in each fiber,

$$\frac{d\langle E_i\rangle}{dz} = 2E_{\text{tot}} - 14\langle E_i\rangle, \quad 0\le i\le 6. \quad (24)$$

Assuming that at $z=0$ all energy is contained in the central fiber, we obtain

$$\langle E_0\rangle = \frac{E_{\text{tot}}}{7}(1+6e^{-14z}),$$

$$\langle E_i\rangle = \frac{E_{\text{tot}}}{7}(1-e^{-14z}), \quad i\ge 1. \quad (25)$$

One can see that an asymptotic state is that of equal energy in all fibers in the array, $\langle E_i\rangle = E_{\text{tot}}/7$. This analysis, and the asymptotic result, can be extended to the full model for an array consisting of 397 fibers packed in 12 layers. One can conclude that equipartition is a statistically preferred state even when the nonlinear contributions can be significant.

VII. CONCLUSIONS

The purpose of this research was to study the competing effects of nonlinearity and randomness in light localization in nonlinear optical fiber arrays. Our analysis leads us to conclude that both nonlinearity and randomness increase the effects of localization in disordered two-dimensional optical fiber arrays. We found that Anderson localization is evident in the linear and intermediate regimes, where a higher fraction of initial energy is returned to the center fiber due to the stochastic effects. The characteristic exponential drop off in energy in the transverse direction is observed. For very high levels of input energy, the system is highly nonlinear and localized and the effects of introducing randomness enhance the localization due to Kerr effects. Finally, the existence of asymptotic localized states and their increased robustness with respect to increased energy levels is also seen in the stochastic model.

Future studies include an analysis of the behavior of optical fiber arrays under different initial states. Of particular interest is a scenario in which input is characterized by broad energy distributions. In such a case, a continuum approximation to the discrete fiber array can be used, which leads to a two-dimensional stochastic nonlinear Schrödinger equation. We intend to study the balance of a blow-up singularity and randomness to determine whether such an initial state can cause localization. Further studies for the long propagation problem described in Sec. VI will also follow, including attempts to deal with the closure problem.

ACKNOWLEDGMENTS

This research was supported by the DOE Office of Science Advanced Scientific Computing Research (ASCR) program in Applied Mathematical Sciences. The authors are thankful to Bruce Robinson, LANL, for many fruitful discussions. The research of A.A. is supported by NSF Grant No. DMS-0505618.

[1] H. S. Eisenberg, Y. Silberberg, R. Morandotti, A. R. Boyd, and J. S. Aitchison, Phys. Rev. Lett. **81**, 3383 (1998).
[2] H. S. Eisenberg, R. Morandotti, Y. Silberberg, J. M. Arnold, G. Pennelli, and J. S. Aitchison, J. Opt. Soc. Am. B **19**, 2938 (2002).
[3] U. Peschel, R. Morandotti, J. S. Aitchison, H. S. Eisenberg, and Y. Silberberg, Appl. Phys. Lett. **75**, 1348 (1999).
[4] U. Peschel, R. Morandotti, J. M. Arnold, J. S. Aitchison, H. S. Eisenberg, Y. Silberberg, T. Pertsch, and F. Ledereret, J. Opt. Soc. Am. B **19**, 2637 (2002).
[5] R. Morandotti, U. Peschel, J. S. Aitchison, H. S. Eisenberg, and Y. Silberberg, Phys. Rev. Lett. **83**, 2726 (1999).
[6] R. Morandotti, H. S. Eisenberg, Y. Silberberg, M. Sorel, and J. S. Aitchison, Phys. Rev. Lett. **86**, 3296 (2001).
[7] J. C. Eilbeck, P. S. Lomdahl, and A. C. Scott, Physica D **16**, 318 (1958).
[8] D. N. Christodoulides and R. I. Joseph, Opt. Lett. **13**, 794 (1988).
[9] A. B. Aceves, G. G. Luther, C. De Angelis, A. M. Rubenchik, and S. K. Turitsyn, Phys. Rev. Lett. **75**, 73 (1995).
[10] A. B. Aceves, C. De Angelis, T. Peschel, R. Muschall, F. Lederer, S. Trillo, and S. Wabnitz, Phys. Rev. E **53**, 1172 (1996).
[11] P. W. Anderson, Phys. Rev. **109**, 1492 (1958).
[12] Y. Lahini, A. Avidan, F. Pozzi, M. Sorel, R. Morandotti, D. Christodoulides, and Y. Silberberg, Phys. Rev. Lett. **100**, 013906 (2008).
[13] A. S. Pikovsky and D. L. Shepelyansky, Phys. Rev. Lett. **100**, 094101 (2008).
[14] T. Schwartz, G. Bartal, S. Fishman, and M. Segev, Nature **446**, 52 (2007).
[15] H. De Raedt, A. Lagendijk, and P. de Vries, Phys. Rev. Lett. **62**, 47 (1989).
[16] J. Topolancik, B. Ilic, and F. Vollmer, Phys. Rev. Lett. **99**, 253901 (2007).
[17] A. A. Asatryan, L. C. Botten, M. A. Byrne, V. D. Freilikher, S. A. Gredeskul, I. V. Shadrivov, R. C. McPhedran, and Y. S. Kivshar, Phys. Rev. Lett. **99**, 193902 (2007).
[18] Y. V. Kartashov, V. A. Vysloukh, and L. Torner, Opt. Express **15**, 19 (2007).
[19] T. Pertsch, U. Peschel, J. Kobelke, K. Schuster, H. Bartelt, S. Nolte, A. Tnnermann, and F. Lederer, Phys. Rev. Lett. **93**, 053901 (2004).
[20] S. M. Jensen, IEEE Trans. Microwave Theory Tech. **82**, 1568 (1982).
[21] C. W. Gardiner, *Handbook of Stochastic Calculus* (Springer, New York, 1985).
[22] H. Risken, *The Fokker-Planck Equation* (Springer, New York, 1999).